Roomtemperature optical absorption in undoped αAl2O3

M. E. Innocenzi, R. T. Swimm, M. Bass, R. H. French, A. B. Villaverde et al.

Related Articles

Optical constants n and κ of various technical and optical glasses at λ=10.59μm
J. Appl. Phys. 113, 013101 (2013)

Efficient terahertz electro-absorption modulation employing graphene plasmonic structures
Appl. Phys. Lett. 101, 261115 (2012)

Spectroscopic imaging ellipsometry and Fano resonance modeling of graphene
J. Appl. Phys. 112, 123523 (2012)

Electrical modulation of the optical properties of mid-infrared metamaterials
Appl. Phys. Lett. 101, 251109 (2012)

Optical properties of metal-dielectric based epsilon near zero metamaterials
Appl. Phys. Lett. 101, 241107 (2012)

Additional information on J. Appl. Phys.

Journal Homepage: http://jap.aip.org/
Journal Information: http://jap.aip.org/about/about_the_journal
Top downloads: http://jap.aip.org/features/most_downloaded
Information for Authors: http://jap.aip.org/authors

Room-temperature optical absorption in undoped α-Al₂O₃

M. E. Innocenzi and R. T. Swimm

Department of Electrical Engineering and Center for Laser Studies, University of Southern California, Los Angeles, California 90089-1112

M. Bass

Department of Electrical Engineering and Physics and the Center for Research on Electrooptics and Lasers, University of Central Florida, Orlando, Florida 32816-0150

R. H. French

E. I. du Pont De Nemours & Company, Inc., Central Research, Wilmington, Delaware 19880

A. B. Villaverde

Instituto de Fisica, Departamento de Electronica Quantica, Universidade Estadual de Campinas, C. P. 6166 Unicamp, 13100-Caminas-S. P., Brazil

M. R. Kokta

Union Carbide Crystal Products Division, 350 South 32nd St., Washougal, Washington 98671

Optical absorption over a large dynamic range obtained by two different experimental techniques is reported for an undoped α-Al₂O₃ single crystal. Absorption data are presented in two energy ranges: 0.94–3.5 eV and 4.5–8.6 eV. Vacuum ultraviolet (vuv) absorption measurements were performed on three boules of Czochralski-grown single-crystal Al₂O₃ with differing starting material purities. The initial powder purities were 99.99%, 99.999%, and 99.999999%. In addition to the vuv measurements, calorimetric absorption results obtained in the visible and near-infrared (ir) are presented. An empirical formula is obtained that provides an estimate of the absorption coefficient from the near-ir to the vuv for undoped Al₂O₃. Detailed impurity analyses and sample histories are given for the optical-quality α-Al₂O₃ utilized herein.

INTRODUCTION

Work on the transparency of white (undoped) α-Al₂O₃ was performed as early as 1939 by Freed, McMurry, and Rosenbaum.[1] In later publications by Gilles *et al.*[2,3] and Romand and Vodar,[4] the first ultraviolet (uv) absorption spectra on pure Al₂O₃ of unknown origin and purity were published. Other early work was performed by Mitchell, Rigden, and Townsend[5] and Heath and Sacher.[6] Mitchell, Rigden, and Townsend[5] reported uv spectra along with some impurity analyses on undoped Al₂O₃ without additional sample history. Heath and Sacher[6] published a uv transmission spectrum for uv-grade Linde Al₂O₃, but no crystal purity or growth information was given. In later work, Il'mas and Kuznetsov[7] published an absorption spectrum for Al₂O₃ from 4.2 to 8.6 eV. Unfortunately, they included no information as to the purity or origin of their "relatively pure" unoriented Al₂O₃. In actuality, their material was quite high in absorption for the 4.2–8.6-eV range. Subsequently, Il'mas, Kuznetsov, and Meriloo[8] presented the most complete study of room-temperature optical absorption in Al₂O₃ up to that time. They presented uv spectra on five pieces of Al₂O₃ along with chemical analyses for three of them. The problem with the study of Il'mas, Kuznetsov, and Meriloo[8] is that two of the three chemical analyses indicate impurity levels that are not consistent with obtainable material purity. Furthermore, one of their samples contained a large concentration of Fe, but did not exhibit a 4.8-eV absorption feature that has been identified as Fe³⁺ by Tippins,[9] Eigenmann, Kurtz, and Günthard,[10] and Blum, Tuller, and Coble.[11]

In reviewing the body of work dealing with optical absorption in the transmissive region of undoped Al₂O₃, most of the work has been limited to the uv region. A complete study, i.e., one with a detailed growth, anneal, and chemical history, on high-quality Al₂O₃ has not yet emerged. The current work represents such a study and presents detailed results that are representative of optical-quality undoped Al₂O₃.

EXPERIMENT

For this work, two different types of experimental studies were performed. In the visible and near-infrared (ir) regions (ir), laser calorimetry was utilized to obtain the absorption coefficient of the Al₂O₃ from 10^{-3} to 10^{-5} cm⁻¹. The calorimetric measurements were performed with several lasers and one calorimeter.[12] The calorimeter was previously employed by Swimm, Xiao, and Bass[13] to perform calorimetric measurements on fused silica. The rate calorimetry data analysis employed in this work is a standard method involving samples of differing length and is described in detail in Ref. 12. In the uv region, relative transmission and reflection measurements were performed to determine the absorption coefficient. The uv spectroscopy required for this work was performed on two different monochromators: a 0.2-m Seya–Namioka vacuum monochromator and a McPherson 225 1-m vacuum monochromator. The 0.2-m monochromator was outfitted with a H₂ lamp as the light source and a vacuum ultraviolet (vuv) windowed photomultiplier tube (PMT) as the detector.[14] The configuration of the normal-incidence 1-m monochromator

(McPherson 225), on which most of the measurements were performed, is described below.[12]

For the 1-m monochromator, the light source was a Hamamatsu L879 deuterium arc lamp[15] and a C1518 lamp power supply. The detector was the Hamamatsu R1460P PMT. The detection electronics consisted of a Hamamatsu C716-02 preamplifier, a C767 photon counter, and a Bertan 205A-05A high-voltage dc supply. For the data obtained on the McPherson 225 monochromator, the maximum entrance and exit slit widths were 65 μm, and the reproducibility of the scan drive was ± 1.5 Å. The MgF$_2$-coated Al grating had a 1200-lines/mm ruling and a blaze wavelength of 1500 Å.

The vuv data taken on the Seya–Namioka monochromator and the normal-incidence monochromator allowed the absorption coefficient α to be determined by three different methods to elucidate agreement between the data obtained from the two different monochromators and to show self-consistency among the analysis methodologies. In cases where both relative transmission (P_t/P_i) and relative reflection (P_r/P_i) data existed, Eqs. (1) and (2) were solved for R and α, the single surface reflectivity and the absorption coefficient, respectively,

$$\frac{P_t}{P_i} = \frac{(1-R)^2 e^{-\alpha L}}{1 - R^2 e^{-2\alpha L}}, \tag{1}$$

$$\frac{P_r}{P_i} = R \left(1 + \frac{(1-R)^2 e^{-2\alpha L}}{1 - R^2 e^{-2\alpha L}} \right), \tag{2}$$

where L is the sample length. In cases where reflection measurements existed on a thin sample with a frosted rear surface, these measurements were combined with transmission measurements from other samples and Eq. (1) was solved directly for the absorption coefficient α. In the event of a back-surface-frosted sample, light striking the rear surface is scattered into nearly 4π steradians; hence, if the detector is positioned far enough from the sample, only the reflection from the front surface is detected. This type of measurement is a good approximation to R, the single-surface reflectivity. In cases where only relative transmission data existed, the transmission of samples of differing length was measured and α was obtained from Eq. (3):

$$\frac{P_{t1}}{P_{t2}} = e^{-\alpha(L_1 - L_2)}. \tag{3}$$

SAMPLE HISTORY

For this work, three pieces of undoped Al$_2$O$_3$ were utilized. The Al$_2$O$_3$ samples will be referred to as samples A, B, and C. The purported purity of the starting materials was 99.999% for sample A, 99.99% for sample B, and 99.999999% for sample C.[16] All three boules are single-crystal Czochralski- (Cz) grown Union Carbide material. The growth parameters that were identical for each case are listed in Table I. Sample B was grown as 0° oriented material. In 0° material, the growth axis, which corresponds to the a axis, is perpendicular to the optic axis (c axis). The starting material was crackle, i.e., chunks of boules grown by the Verneuil method. Samples A and C were grown as 60° oriented mate-

rial. In actuality, the growth axis corresponds to the r plane, which is 59.6° from the c axis. For the sample A sapphire, the starting material was an ingot of isostatically pressed Al$_2$O$_3$ powder. The starting material in the sample C case was loose Al$_2$O$_3$ powder. Samples A and B underwent a post-growth vacuum anneal whereas sample C was measured unannealed. The anneal parameters are summarized in Table II.

Impurity analyses were performed on samples A and B. Samples of these boules were sent to Northern Analytical Laboratory[17] for spark source mass spectrography (SPSS). Trace impurity analysis on control samples sent to this laboratory by Tebbe et al.[18] have been found to be within a factor of 2 of the known impurity concentration for 65% of the analyses and within a factor of 3 for 85% of the analyses. For example, samples with known concentrations of Fe have been analyzed to contain 50% of the actual Fe concentration. In the case of sample C, only the starting material (Al$_2$O$_3$ powder) was analyzed. This analysis was done using the inductively coupled plasma (ICP) technique at Ceralox Corporation.[19] The results of all three analyses are tabulated in Table III. These analyses show that the actual purity of samples A and B and the sample C starting material is 99.99%. In addition to the starting material impurities, sample C may contain impurities that entered during the growth process.[20]

The sample processing for the A and C material was done at Aerospace Corporation[21] and Laser Power Optics (LPO).[22] As a first step, the boules were oriented using x-ray diffraction and cut with the c axis perpendicular to the sample faces. Then the samples were sent to LPO where they underwent chemical polishing. As an alternate, some of the samples were chemically polished at Dupont[23] and were of comparable quality to those polished at LPO. The remaining sample, B, existed from previous calorimetric measurements.[24] Again, this sample was oriented with the c axis perpendicular to the sample faces. Sample B received a high-quality optical polish comparable to that received by the rest of the Al$_2$O$_3$.

RESULTS AND DISCUSSION

As a precursor to the transmission measurements, a qualitative scattering test was conducted on the Al$_2$O$_3$ sam-

TABLE I. Growth parameters for the Al$_2$O$_3$ boules.

Atmosphere	N$_2$ + 800 ppm O$_2$
Pull rate	0.125 in./h
Rotation rate	15–20 rpm
Crucible	iridium
Temperature (at seed)	2050 °C

TABLE II. Anneal parameters for the Al$_2$O$_3$ boules.

Temperature	1980 °C
Duration	40 h
Cooling rate	80–100 °C/h

TABLE III. Results of the Al_2O_3 chemical analyses. Impurity concentrations are in ppmw and ppma. The former is a ratio of the atomic weight of the impurity to the average atomic weight of Al_2O_3 and the latter is the number of impurity atoms per million atoms of Al_2O_3. The < and ⩽ relation signs are present at the detection limits and where possible interference from molecular clusters of the same weight may have occurred. The pregrowth powder for sample c was analyzed using optical ICP at Ceralox Corporation. Samples A and B (after growth) were analyzed using SSMS at Northern Analytical Laboratory. For samples A and B, elements not reported are less than 0.02 ppma nominal, which is the detection limit for these analyses. Generally, for elements with more than one isotope, the ppma nominal is corrected by the abundance factor for the most abundant isotope. As an example, for Ni, the detection limit becomes 0.03 ppma, i.e., 0.02 ppma nominal x (1.0/0.6827), where 0.6827 is the isotropic abundance of Ni^{58}.

Name Impurity	Sample A	Sample B	Sample C	Sample A	Sample B	Sample C
	Concentration (ppmw)			Concentration (ppma)		
	Sample A	Sample B	Sample C	Sample A	Sample B	Sample C
Si	⩽6	⩽6	70	⩽4	⩽4	51
Ga	0.7	0.3	<4	0.2	0.1	<1.2
Mo	...	...	<4	...	...	<0.9
Na	0.5	0.3	<4	0.4	0.3	<3.5
Ca	2	1	3	1	0.7	1.5
Fe	0.8	0.6	2	0.3	0.2	0.7
Mg	<3	<3	2	<2	<2	1.7
Zr	...	...	2	...	...	0.5
Cr	⩽0.8	⩽0.8	<1	⩽0.3	⩽0.3	<0.4
Cu	⩽0.1	⩽0.1	<1	⩽0.04	⩽0.04	<0.3
Ni	⩽0.1	⩽0.1	<1	⩽0.04	⩽0.04	<0.4
Mn	...	...	<1	...	...	<0.4
Ti	...	...	<1	...	...	<0.4
Zn	...	...	<1	...	...	<0.3
Li	...	...	<1	...	...	<3
Cl	7	5	...	4	3	...
S	<3	⩽3	...	<2	⩽2	...
K	0.4	0.4	...	0.2	0.2	...
P	0.08	0.05	...	0.05	0.03	...

ples to determine whether they contained internal scattering centers. To facilitate this measurement, Ar^+ and Kr^+ lasers were employed as optical probes and a visual examination of the samples was performed. Within the limits of this crude measurement, no scattering centers were detected in the sample B Al_2O_3. In contrast, in the A and C material, a distinct filament of scattering centers could be seen along the laser beam path. Since the sample B material was grown from crackle, the appearance of scattering centers was minimized.

As a second diagnostic, all of the samples were scanned on a spectrophotometer before and after the uv absorption measurements. This was done to ensure that additional absorptions did not occur at the near-ir, visible, or uv wavelengths, which would indicate color-center formation in the samples. No changes in the spectrophotometer transmission characteristics were detected.

Figure 1 displays uv absorption spectra for the three boules of Cz-grown undoped Al_2O_3. Sample A is represented by the circles, sample B by the squares, and sample C by the triangles. A representative error bar, calculated at one standard deviation, is also displayed in Fig. 1. This error bar encompasses all experimental uncertainties including differences among samples of the same material. The actual error bars for the sample B uv measurements, which are depicted in Fig. 2, are somewhat less than this representative error bar. The absorption data of Fig. 1 was generated using eight pieces of sample A material, six pieces of sample B material, and four pieces of sample C material. As can be seen from Fig. 1, there are several broad absorption features in the spectra that are characteristic of charge transfer[9] that occurs between O^{2-} ligands and transition-metal ions of valency $3+$. Employing Fig. 1 and Table III, it is interesting to compare the overall chemical analysis of samples A and B to their optical spectra. The chemical analysis indicates that the sample A material has, in all cases, greater trace impurity content or the same trace impurity content as the sample B material. It is evident that the chemical analysis alone will not elucidate the cause of the optical absorption differences between samples A and B. This effect may be due, in part, to uncertainties in the actual impurity concentrations as was discussed in the section on sample history.

Beyond 8.5 eV, all of the crystals begin to increase in absorption as they begin to track the onset of the fundamental absorption in Al_2O_3. The transmission of all samples went to 0.0 at 8.75 eV. This energy is close to the 8.8-eV estimate of the room temperature optical band gap given by French[14] and many of the references cited by Arakawa and
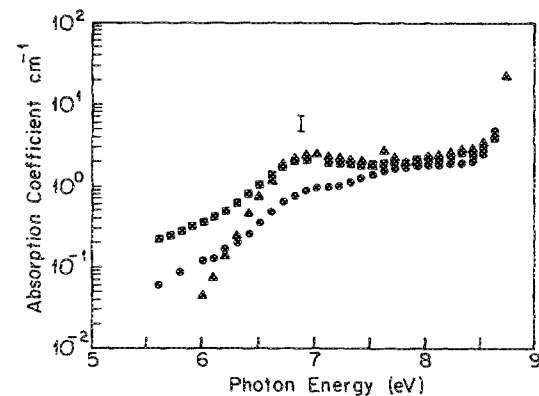

FIG. 1. uv absorption spectra for the three boules of Cz-grown undoped Al_2O_3. Sample A is represented by the circles, sample B by the squares, and sample C by the triangles.

Williams,[25] although they estimated the band edge to be at 8.55 eV. In Fig. 1, one absorption feature is readily observable in all three spectra. This is the absorption band centered at 7.0 eV. At 7.0 eV, absorptions have been attributed to Cr by Loh,[26] Cr, Ni, and Fe (7.2 eV) by Tippins,[9] and an anionic vacancy by Il'mas, Kuznetsov, and Meribo.[8] In addition, Lee and Kröger[27] have reported a donor level for Si in polycrystalline Al_2O_3 near 7.0 eV (1.7 eV from the valence band edge), but this has not been observed in optical measurements. In the present study, all of the crystals display 7.0 eV absorption and contain Cr, Fe, and Ni, but for samples A and B, Ni is present at a concentration that is almost an order of magnitude less than the Cr and Fe concentrations.

Continuing with Fig. 1, in the case of the sample A spectrum (circles), two additional absorption features can be discerned. The first absorption band is centered at approximately 8.0 eV. Absorptions in the vicinity of 8.0 eV have been attributed to Cr (7.8 and 8.3 eV) by Loh[26] and Mn (8.0 eV) by Tippins.[9] The second absorption feature occurs in the vicinity of 6.0 eV. Absorption near 6.0 eV has also been associated with Mn by Tippins.[9] In samples that were not reported to contain Mn, Mitchell, Rigden, and Townsend[5] suggested that a possible cause of the 6.0-eV absorption was an interstitial Al decorated with an e^-. From Table III, the sample A material was found to contain Cr (<0.8 ppmw) but not Mn. From this, it can be concluded that the 8.0- and 6.0-eV absorptions in the sample A spectrum are most probably not due to Mn.

The next feature observed in this study, the 4.8-eV absorption band, is shown in Fig. 2. Figure 2 displays uv and calorimetric absorption results for sample B. The uv data extend from 8.6 to 4.5 eV and the calorimetry data from 3.5 to 0.9 eV. Both types of Fig. 2 data were generated from the same six pieces of sample B material utilized for the data of Fig. 1. The uv error bars are computed at one standard deviation while the calorimetric error bars are derived from a statistically weighted least-squares fit of the absorption data at each wavelength. Absorption at 4.8 eV has been associated with the presence of Fe by Tippins,[9] Eigenmann, Kurtz, and Günthard,[10] and Blum, Tuller, and Coble,[11] and to Cr and V by McClure.[28] The only crystal that was measured in the 4.8-eV region, sample B, contains Fe and Cr, but does not contain V. The remaining absorption at 3.0 eV, which is observed in the sample B calorimetric results, is probably due to the presence of Cr since Cr absorption at 3.1 eV has been reported by McClure[28] and others. McClure also reported a 3.1 eV absorption due to V, but V is not present in the sample B material.

From the combination of the uv absorption data and the calorimetric results (Fig. 2), a simple empirical relation can be written to obtain an approximate value for the absorption coefficient of undoped Al_2O_3 over four decades of magnitude (1.0×10^{-4} to 1.0 cm^{-1}). This empirical relation can be employed as an order of magnitude estimate of the optical absorption in undoped Al_2O_3. It is written as

$$\alpha = 10^{-4.5} \text{ cm}^{-1} \times 10^{E[\text{eV}]/1.7\text{ eV}}, \qquad (4)$$

where α is the absorption coefficient in cm^{-1}, and E is the photon energy in eV. Equation (4) is applicable for photon
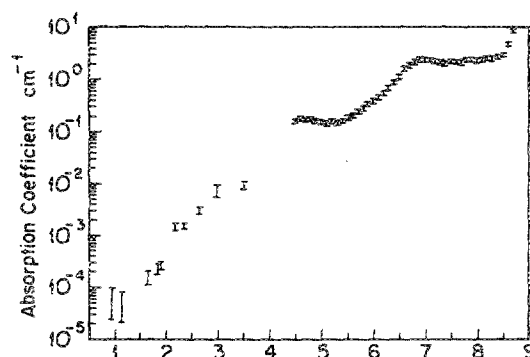

FIG. 2. uv and calorimetric absorption results for sample B. The uv data extend from 8.6 to 4.5 eV and the calorimetry data from 3.5 to 0.9 eV. The uv error bars are computed at one standard deviation while the calorimetric error bars are derived from a statistically weighted least-squares fit of the absorption data at each wavelength.

energies from 0.9 to 8.5 eV. Since a temperature-dependent study of optical absorption was not performed, an Urbach model[29,30] was not assumed for the absorption coefficient.

CONCLUSION

uv absorption spectra have been obtained for three different boules of undoped Cz-grown optical-quality Al_2O_3 along with calorimetric absorption measurements on one of the boules. An empirical formula has been obtained that provides an estimate of the absorption coefficient from the visible to the vuv regions for undoped Al_2O_3. Along with the absorption measurements, detailed chemical analyses were performed on all three boules of material and compared to the optical spectra. In the Al_2O_3 absorption spectra, absorption features were seen at 8.0, 7.0, 6.0, 4.8, and 3.1 eV. From previously reported results, most of the absorption bands can be attributed to trace impurities. From the uv absorption measurements, it is clear that Al_2O_3 absorption in the uv region is heavily influenced by extrinsic defects. At present, these impurity absorptions cannot be separated out to obtain the intrinsic crystalline absorption. Additional controlled doping studies like that performed by Loh[26] are required to obtain absorption cross sections for ubiquitous impurities in Al_2O_3. Cross-sectional studies along with detailed trace impurity analyses are necessary to help isolate extrinsic absorption effects from those due to intrinsic mechanisms. Although the optical quality of single-crystal Al_2O_3 has improved, the uv absorption characteristics have not changed appreciably since the work of Gilles et al.[2] in 1947.

To help reduce uv absorption levels, additional work is required to develop higher-purity starting materials such as that reported by Tebbe et al.[18] Moreover, since the overall uv absorption levels have not changed considerably in 42 years, this may represent a plateau that may not be improved upon by conventional technology. Alternate growth techniques that share a higher degree of cleanliness, such as laser float-zone growth,[31] could represent part of the solution.

[1] S. Freed, H. L. McMurry, and E. J. Rosenbaum, J. Chem. Phys. 7, 853 (1939).

[2] A. Gilles, R. Bauplé, J. Romand, and B. Vodar, C. R. Acad. Sci. 229, 876 (1947).

[3] A. Gilles, J. Phys. Radium 13, 247 (1952).

[4] J. Romand and V. Vodar, Spectrochim. Acta 8, 229 (1956).

[5] W. J. Mitchell, J. D. Rigden, and P. D. Townsend, Philos. Mag. 5, 1013 (1960).

[6] D. F. Heath and P. A. Sacher, Appl. Opt. 5, 937 (1966).

[7] É. R. Il'mas and A. I. Kuznetsov, Sov. Phys. Solid State 14, 1255 (1972).

[8] É. A. Il'mas, A. I. Kuznetsov, and I. A. Meriloo, J. Appl. Spectrosc. (USSR) 24, 459 (1976).

[9] H. H. Tippins, Phys. Rev. B 1, 126 (1970).

[10] K. Eigenmann, K. Kurtz, and Hs. H. Günthard, Helv. Phys. Acta 45, 452 (1972).

[11] J. B. Blum, H. L. Tuller, and R. L. Coble, J. Am. Ceram. Soc. 65, 379 (1982).

[12] M. E. Innocenzi, Ph.D. thesis, University of Southern California, Los Angeles, CA (1989), available from University Microfilms, Ann Arbor, MI.

[13] R. T. Swimm, Y. Xiao, and M. Bass, Appl. Opt. 24, 322 (1985).

[14] R. H. French, Ph.D. thesis, MIT, Cambridge, MA (1985), available from University Microfilms, Ann Arbor, MI; see also *Advanced Characterization Techniques for Ceramics*, Vol. 5 of *Ceramic Transactions*, edited by W. S. Young, G. L. McVay, and G. E. Pike (American Ceramic Society, Westerville, OH, 1989), p. 406.

[15] Hamamatsu Corp., 420 South Ave., Middlesex, NJ.

[16] The stated purity of the starting materials is based on the total cation impurity content by weight. For example, a 99.99% pure Al_2O_3 powder should contain 999.9 g of pure Al_2O_3 and no more than 0.1 g of all cation impurities per 1000 g of powder. For the 99.99% case, this would be equivalent to a cation impurity content of no more than 100 ppmw, where ppmw is parts per million by weight.

[17] Northern Analytical Laboratory, Inc., Amherst, NH. In their analysis, the Al_2O_3 and high-purity graphite is ignited in the spark source and then mass spectroscopy is performed on the resultant species.

[18] F. M. Tebbe, P. A. Morris, R. H. French, U. Chowdhry, and R. L. Coble, J. Am. Ceram. Soc. 71, C-204 (1988).

[19] Ceralox Corp., 7800 South Kolb Rd., Tucson, AZ. The ICP method entails igniting the constituents in a plasma flame and then analyzing the resultant species optically or with a mass spectrometer.

[20] It should immediately be pointed out that neither sample C nor its starting material was expected to be truly 99.9999999%, i.e., having a total cation impurity content of no more than 0.01 ppmw. As is established by the ICP analysis in Table III, the sample C starting material is 99.99% pure.

[21] The Aerospace Corp., P.O. Box 92957, Los Angeles, CA.

[22] Laser Power Optics, 12777 High Bluff Dr., San Diego, CA.

[23] E. I. du Pont De Nemours & Company, Inc., Central Research and Development Dept., Experimental Station, Wilmington, DE.

[24] A. B. Villaverde, R. T. Swimm, and M. Bass, *Boulder Damage Symposium Proceedings*, NBS Spec. Publ. 697, 1985, p. 164.

[25] E. T. Arakawa and M. W. Williams, J. Phys. Chem. Solids 29, 735 (1968).

[26] E. Loh, J. Chem. Phys. 44, 1940 (1966).

[27] C. H. Lee and F. A. Kröger, J. Am. Ceram. Soc. 68, 92 (1985).

[28] D. S. McClure, J. Chem. Phys. 36, 10 (1962).

[29] F. Urbach, Phys. Rev. 92, 1324 (1953).

[30] J. D. Dow and D. Redfield, Phys. Rev. B 5, 594 (1972).

[31] P. A. Morris, in *Sintering of Advanced Ceramics*, Vol. 7 of *Ceramic Transactions*, edited by C. A. Hondwerker, J. E. Blendell, and W. Kaysser (American Ceramic Society, Westerville, OH, 1990) p. 50.